

## Synthesis and structure-mechanical property correlation of an $\alpha,\beta$ -hybrid peptide containing methyl-3-aminocrotonate

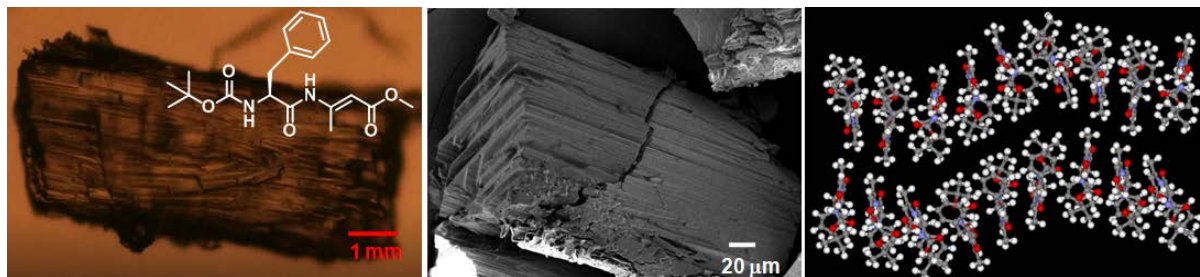
Santosh Kumar, Debasish Haldar\*

Department of Chemical Sciences, Indian Institute of Science Education and Research Kolkata, Mohanpur-741246, West Bengal, India.

Submitted on: 10-Feb-2022, Accepted and Published on: 4-Mar-2022

Article

### ABSTRACT



An  $\alpha,\beta$ -hybrid peptide has been synthesized and the structure-mechanical property correlation of the peptide has been presented. The  $\alpha,\beta$ -hybrid peptide **1** has L-Phe and methyl-3-aminocrotonate residues and formed monoclinic crystals, with space group P 21/n. The X-ray crystallography analysis indicate that there is a five-member  $\text{NH}\cdots\text{N}$  and a six-member intramolecular  $\text{NH}\cdots\text{O}=\text{C}$  hydrogen bond and the  $\alpha,\beta$ -hybrid peptide **1** adopts a turn-like conformation, due to the *E* geometry of the methyl-3-aminocrotonate residue. The  $\alpha,\beta$ -hybrid peptide **1** molecules self-assemble by intermolecular  $\text{N-H}\cdots\text{O}$  hydrogen bonds and form a supramolecular twisted sheet-like structure which further assembled to form a supramolecular multi layered structure along the crystallographic *b* and *c* directions. However, the  $\alpha,\beta$ -hybrid peptide **1** crystals are sensitive to external stress and brittle in nature. From FE-SEM image, the crystal appears as a layer-by-layer structure. The intermolecular interaction energies (kJ/mol) for the  $\alpha,\beta$ -hybrid peptide **1** were calculated using B3LYP/6-31G(d,p) dispersion corrected DFT model. Although the interaction energy is small, there is no scope of slippage due to the interaction of the Boc-*t*-butyl, Phe side chains and methyl-3-aminocrotonate in the multi layer sheets.

**Keywords:**  $\alpha,\beta$ -hybrid peptide, *E* geometry, brittle crystal, methyl-3-aminocrotonate, sheet-like structure

### INTRODUCTION

The higher order packing combined with strong intermolecular interactions make organic single crystals as excellent candidates for electron export and mechanical actuation.<sup>1-5</sup> Recently, organic crystals have found application in ferroelectricity,<sup>6</sup> waveguides,<sup>7-8</sup> and field-effect transistors for ultrasensitive strain sensing.<sup>9</sup> However, most of the organic crystals are fragile and are inferior to thin films and liquid crystals in terms of mechanical flexibility. On exposure to external impetus such as heat, humidity, light<sup>10</sup> and mechanical stress, the organic crystals may bend,<sup>11</sup> twist,<sup>12</sup> curl,<sup>13</sup> or ruptured.<sup>14-15</sup> The structure-mechanical property correlation of organic crystals depends on factors like

hierarchical organization at supramolecular or macroscopic levels.<sup>16</sup> For crystal engineering, the understanding, controlling, and designing such mechanical properties in organic crystals are highly important.<sup>17-18</sup> Generally, the weak intermolecular interactions like van der Waals interactions,  $\pi$ - $\pi$  stacking, hydrogen bonding are key to introduce slip planes within the mechanically bendable crystals.<sup>19</sup> In a recent review, Reddy and his co-workers have noted the mechanical responses of organic crystals.<sup>20</sup> Ramamurty has reported the use of nanoindentation to examine the mechanical properties of organic crystal.<sup>21</sup> Gabriele and co-workers have discussed the brittle behavior of aspirin crystals.<sup>24</sup>

In this regard, herein we have synthesized an  $\alpha,\beta$ -hybrid peptide **1** containing L-phenylalanine (Phe) and methyl-3-aminocrotonate and wanted to investigate the structure-mechanical property correlation. From solid state structure, there is a six-member intramolecular hydrogen bond and  $\alpha,\beta$ -hybrid peptide **1** adopts a turn-like conformation. The methyl-3-aminocrotonate residue has *E* geometry. The  $\alpha,\beta$ -hybrid peptide **1** molecules self-assemble by intermolecular  $\text{N-H}\cdots\text{O}$  hydrogen bonds and form a supramolecular twisted sheet-like structure which further assembled to form a supramolecular multi layers

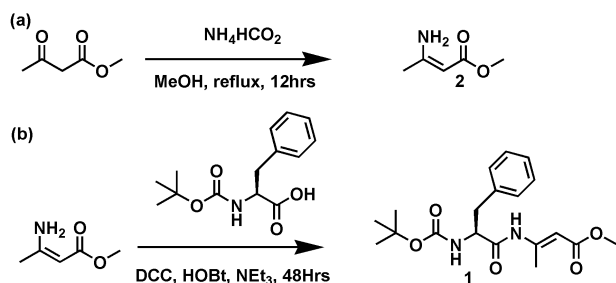
\*Corresponding Author: Dr. Debasish Haldar  
Department of Chemical Sciences, Indian Institute of Science Education and Research  
Kolkata, Mohanpur-741246, West Bengal, India  
Email: deba\_h76@iiserkol.ac.in



structure. The  $\alpha,\beta$ -hybrid peptide **1** crystals are sensitive to external stress and brittle in nature. From electron microscopy the crystal appears as a layer by layer structure. Eventually, the intermolecular interaction energies (kJ/mol) for the  $\alpha,\beta$ -hybrid peptide **1** were calculated using B3LYP/6-31G(d,p) dispersion corrected DFT model. Though the interaction energy is small, there is no scope of slippage due to the interaction of the Boc-*t*-butyl, Phe side chains and methyl-3-aminocrotonate in the multi layer sheets.

## RESULTS AND DISCUSSION

We have developed an unsaturated amino acid methyl-3-aminocrotonate by refluxing methylacetoacetate with ammoniumformate in methanol for 12 hours (Scheme 1a) with 68% yield. The terminally protected  $\alpha,\beta$ -hybrid peptide **1** containing L-phenylalanine(Phe) and methyl-3-aminocrotonate was synthesized by conventional solution-phase peptide synthesis method using *N,N'*-dicyclohexylcarbodiimide (DCC) as coupling agent. *N*-hydroxybenzotriazole (HOBt) has been used to improve the efficiency of peptide synthesis and suppress the racemization of L-Phe (Scheme 1b).<sup>23-24</sup> The  $\alpha,\beta$ -hybrid peptide **1** backbone has internal rigidity due to *E*-geometry of the methyl-3-aminocrotonate. The synthesized compounds were purified by column chromatography and characterized by <sup>1</sup>H-NMR, <sup>13</sup>C-NMR, FT-IR spectroscopy, and mass spectrometry (MS).



**Scheme 1.** (a) Synthesis of methyl-3-aminocrotonate. (b) Synthesis of the  $\alpha,\beta$ -hybrid peptide **1** by solution method.

The aggregation behavior of the  $\alpha,\beta$ -hybrid peptide **1** has been investigated by UV-Vis and fluorescence spectroscopy. The  $\alpha,\beta$ -hybrid peptide **1** shows absorption bands at 272nm (Supporting Information Figure S1). With increase in the concentration of  $\alpha,\beta$ -hybrid peptide **1**, the respective absorption band does not show any shift; only intensity increases gradually. The  $\alpha,\beta$ -hybrid peptide **1** shows emission spectra at 340 nm upon excitation at 272 nm (Supporting Information Figure S2). The fluorescence intensity increases with the increasing concentration of the  $\alpha,\beta$ -hybrid peptide **1**.

To know the conformation of  $\alpha,\beta$ -hybrid peptide **1** in solid state, FT-IR spectroscopy was performed. The  $\alpha,\beta$ -hybrid peptide **1** shows an intense band at  $3338\text{ cm}^{-1}$  for non hydrogen-bonded NH's (Figure 1). A band at  $1720\text{ cm}^{-1}$  is responsible for the ester C=O. The amide I and amide II bands appeared at 1660 and 1508

$\text{cm}^{-1}$  (Figure 1) respectively indicating the presence of kink-like conformation.<sup>26</sup>

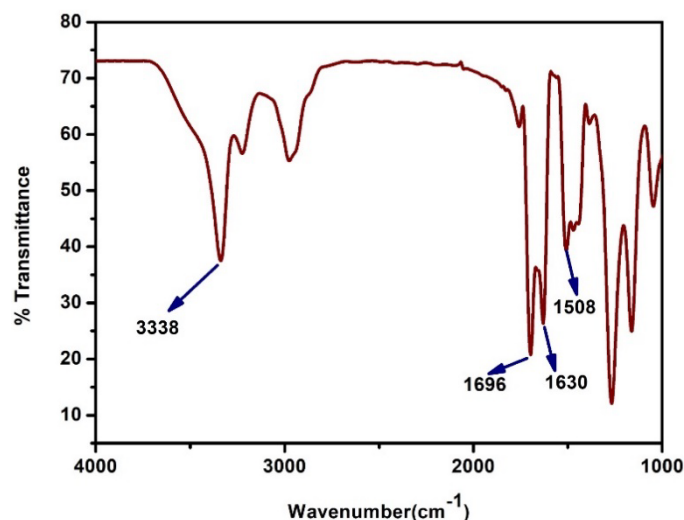


**Figure 1.** Solid state FT-IR spectra of  $\alpha,\beta$ -hybrid peptide **1**.

The pure  $\alpha,\beta$ -hybrid peptide **1** was subjected to crystallization from methanol-water solution at room temperature by slow evaporation. The monoclinic crystals are very sensitive to external stress and brittle in nature. Using needle and forceps, crystals of the  $\alpha,\beta$ -hybrid peptide **1** were subjected to mechanical stress (Figure 2a), under the optical microscope. Crystals of  $\alpha,\beta$ -hybrid peptide **1** were fractured into pieces (Figure 2b) on the application of mechanical stress at room temperature.

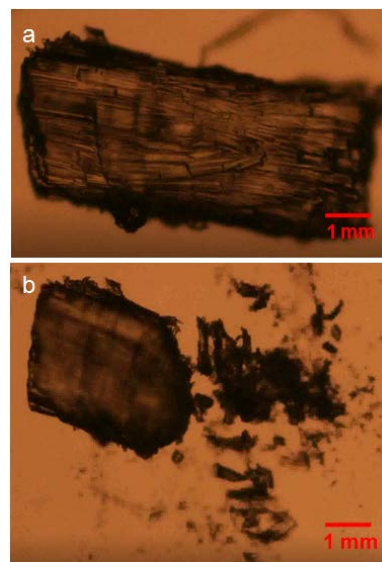


**Figure 2.** (a) External stress on the crystal of  $\alpha,\beta$ -hybrid peptide **1**. (b) The  $\alpha,\beta$ -hybrid peptide **1** crystal breaks down and pieces of the brittle crystal.

Further the nature of the mechanically broken surface of the crystals of  $\alpha,\beta$ -hybrid peptide **1** was studied by the Field emission scanning electron microscopy (FE-SEM). The crystals as well as

the debris of broken crystal were investigated by FE-SEM. At higher magnification, the analysis of the morphology of  $\alpha,\beta$ -hybrid peptide **1** by FE-SEM shows that the crystal has a layer by layer assembly morphology (Figure 3a). From the broken end of the crystal of the  $\alpha,\beta$ -hybrid peptide **1** (Figure 3b), the crystal is actually a thick bundle of several sheet like structure.

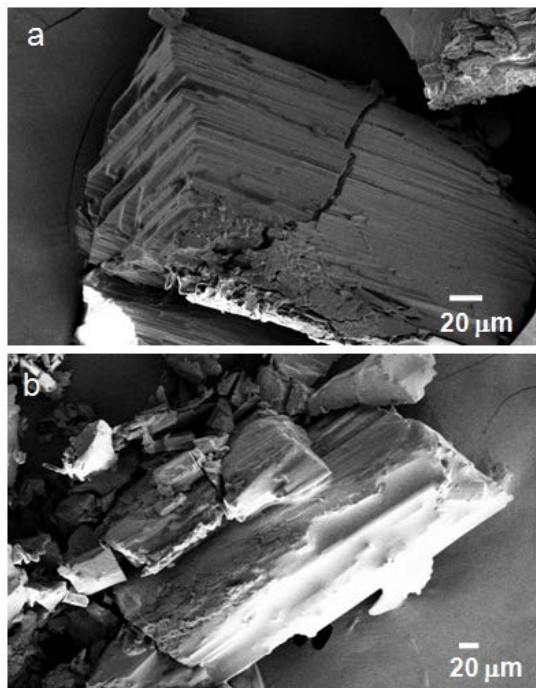


**Figure 3.** (a) FE-SEM image showing layer by layer morphology of the  $\alpha,\beta$ -hybrid peptide **1** crystal. (b) The debris of dipeptide **1** crystal showing multi layer structure.

The  $\alpha,\beta$ -hybrid peptide **1** was also characterized by single-crystal X-ray diffraction analysis. From X-ray crystallography, the  $\alpha,\beta$ -hybrid peptide **1** crystallizes with three molecules in the asymmetric unit (Supporting Information Figure S3). Two molecules are in parallel orientation and third one is in anti-parallel fashion. By looking at, it would appear that the dihedral angles around L-Phe residue are  $\phi_1 = -111.07^\circ$  and  $\psi_1 = 13.35^\circ$  for molecule A;  $\phi_1 = -112.54^\circ$  and  $\psi_1 = 25.72^\circ$  for molecule B and  $\phi_1 = -113.01^\circ$  and  $\psi_1 = 12.95^\circ$  for molecule C. The torsion angles around methyl-3-aminocrotonate residue are  $\phi_2 = -168.33^\circ$ ,  $\theta_2 = -1.12^\circ$  and  $\psi_2 = 176.65^\circ$  for molecule A;  $\phi_2 = 176.14^\circ$ ,  $\theta_2 = 2.09^\circ$  and  $\psi_2 = 177.98^\circ$  for molecule B;  $\phi_2 = -172.24^\circ$ ,  $\theta_2 = -1.18^\circ$  and  $\psi_2 = 174.79^\circ$  for molecule C.<sup>30</sup> From Figure 4a, it is clear that the  $\alpha,\beta$ -hybrid peptide **1** adopts a turn-like structure and stabilized by an unusual six member hydrogen bond between methyl-3-aminocrotonate C=O and NH and five member hydrogen bond between Phe N and methyl-3-aminocrotonate NH (Figure 4a). Three molecules in the asymmetric unit are also stabilized by inter molecular NH $\cdots$ O=C hydrogen bonds and  $\pi$ - $\pi$  stacking interactions. The  $\alpha,\beta$ -hybrid peptide **1** molecules further self-assembled to form a twisted sheet-like structure stabilized by multiple intermolecular N-H $\cdots$ O hydrogen bonds (Figure 4b). The hydrogen bonding

parameters of the  $\alpha,\beta$ -hybrid peptide **1** are listed in Table 1. There is also  $\pi$ - $\pi$  stacking interaction between molecules that are in parallel orientation (shortest C-C distance is 3.63 Å). Crystal parameters are listed in Supporting Information Table S1.

**Table 1.** Hydrogen bonding parameters of  $\alpha,\beta$ -hybrid peptide **1**.<sup>[a]</sup>

D-H $\cdots$ A	D $\cdots$ H(Å)	H $\cdots$ A(Å)	D $\cdots$ A(Å)	D-H $\cdots$ A( $^\circ$ )
N1-H1 $\cdots$ O12 <sup>a</sup>	0.88	2.06	2.875(6)	155
N2-H2 $\cdots$ O4	0.88	1.98	2.694(7)	137
N3-H3 $\cdots$ O2	0.88	2.08	2.828(3)	142
N4-H4 $\cdots$ O9	0.86	2.00	2.705(7)	137
N5-H5 $\cdots$ O7	0.88	2.03	2.853(6)	155
N6-H6 $\cdots$ O14	0.88	2.01	2.706(7)	135
N2-H2 $\cdots$ N1	0.88	2.25	2.711(6)	112
N4-H4 $\cdots$ N3	0.88	2.34	2.755(8)	109
N6-H6 $\cdots$ N5	0.88	2.24	2.709(8)	113

<sup>[a]</sup> Symmetry equivalent:  $a = 3/2-x$ ,  $-1/2+y$ ,  $1/2-z$ .

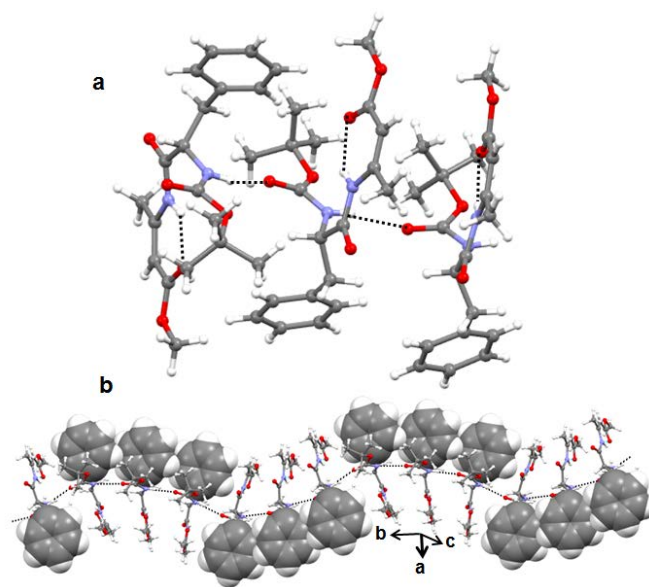


**Figure 4.** (a) The solid-state structure of  $\alpha,\beta$ -hybrid peptide **1** showing intra and inter molecular hydrogen bonds in asymmetric unit.; (b) Intermolecular hydrogen bonded twisted sheet-like structure of  $\alpha,\beta$ -hybrid peptide **1**. Intramolecular hydrogen bonds are shown as dotted lines.

In higher-order, the  $\alpha,\beta$ -hybrid peptide **1** molecules further self-assembled to form multi layer sheet-like structure, though there is no hydrogen bonds or  $\pi$ - $\pi$  stacking interaction between the sheets (Figure 5a). From the surface diagram (Figure 5b), the hydrophobic interactions between two sheets are not continuous, rather there are weak zones periodically between two sheets along the crystallographic  $a$  and  $c$  direction. Also there is no scope of slippage due to wavy nature of the multi layer sheets, which may be responsible for the brittleness of the  $\alpha,\beta$ -hybrid peptide **1** crystal.



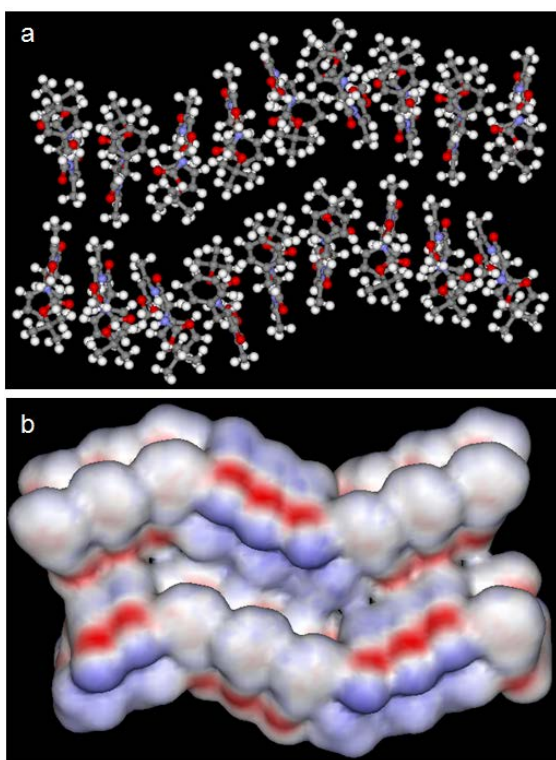


**Figure 5.** (a) The self-assembled multi layer twisted sheet-like structure of  $\alpha,\beta$ -hybrid peptide **1**. (b) The surface diagram of multi layer twisted sheet of  $\alpha,\beta$ -hybrid peptide **1**.

Moreover, we have analyzed the Hirshfeld surfaces (HSs) for the  $\alpha,\beta$ -hybrid peptide **1** and related 2D fingerprint plots (FPs).<sup>27</sup> Hirshfeld surfaces maps of the  $\alpha,\beta$ -hybrid peptide **1** exhibited some red region which refers to the intermolecular H-bonding interactions (Figure 6a). A visual summary of the frequency of each combination of  $d_e$  and  $d_i$  across  $\alpha,\beta$ -hybrid peptide **1** surface (the 2D fingerprint plot) exhibits that both hydrogen bonding interactions and H...H intermolecular contacts have significant contribution toward intermolecular interactions (Figure 6b, c, d, e). The H...H interactions appeared as scattered spikes in the 2D fingerprint plots with overall Hirshfeld surfaces of 64.4%. The contribution from the O...H contacts is 18.1%, contribution from the C...H contacts is 14.7% and contribution from the N...H contacts is 1.6% and other minor contributions due to C...O (0.6%), O...N (0.4%), C...C (0.2%).

Moreover, we have used CrystalExplorer, 21.5 for the quantification of pairwise total intermolecular interaction energies of  $\alpha,\beta$ -hybrid peptide **1**. This can bring forth a quantitative explanation of the intermolecular energy, related mechanical behavior and identification of the active slip plane in the crystal structures of  $\alpha,\beta$ -hybrid peptide **1**.<sup>28–30</sup> For the  $\alpha,\beta$ -hybrid peptide **1**, the intermolecular interaction energies (kJ/mol) was calculated using B3LYP/6-31G(d,p) dispersion corrected DFT model. The X–H bond lengths was normalized to standard neutron diffraction values. The exchange-repulsion ( $E_{rep}$ ), total energy ( $E_{tot}$ ), polarization ( $E_{pol}$ ), dispersion ( $E_{dis}$ ) and electrostatic ( $E_{ele}$ ) components of the energy are listed in Supporting Information Table S2. The magnitude of calculated energies

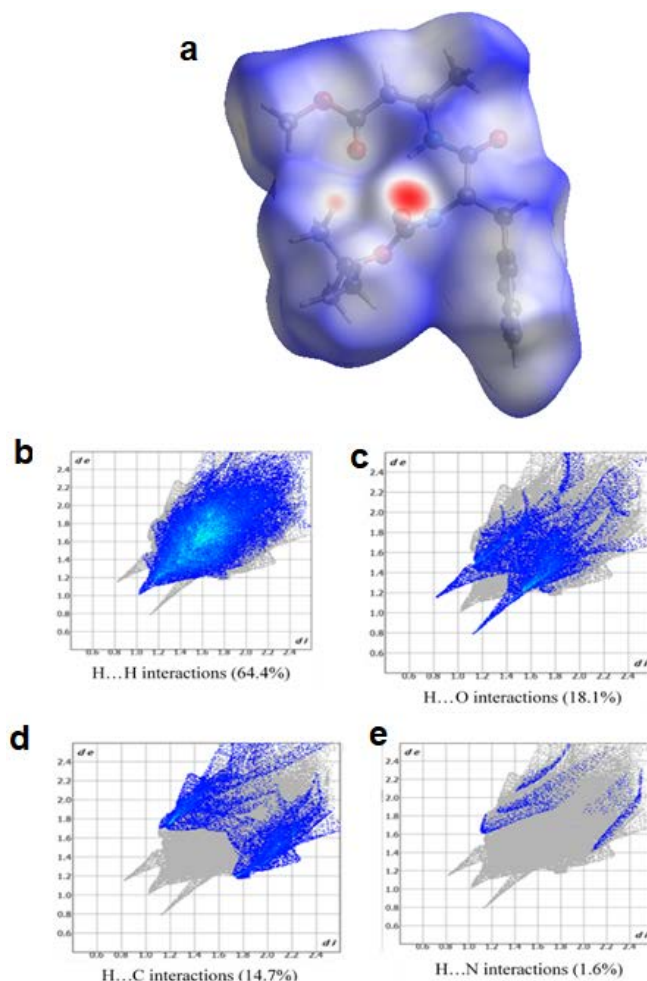


**Figure 6.** (a) The Hirshfeld surfaces maps of the  $\alpha,\beta$ -hybrid peptide **1**. (b) The 2D fingerprint plot of  $\alpha,\beta$ -hybrid peptide **1** for H...H interactions. (c) The 2D fingerprint plot of  $\alpha,\beta$ -hybrid peptide **1** for H...O interactions. (d) The 2D fingerprint plot of  $\alpha,\beta$ -hybrid peptide **1** for H...C interactions. (e) The 2D fingerprint plot of  $\alpha,\beta$ -hybrid peptide **1** for H...N interactions.

among molecular pairs of  $\alpha,\beta$ -hybrid peptide **1** was presented as cylinders of proportionate thickness connecting the centers of mass (Figure 7 and Supporting Information Figure S4). Total interaction energies of the molecule were calculated within 3.8 Å (Supporting Information Figure S5). However, the 3D topologies of the energy framework of  $\alpha,\beta$ -hybrid peptide **1** show that each molecule is surrounded by 7 closest neighbors across alkyl slip planes (Supporting Information Figure S5). The energy distribution is not isotropic and different in different directions which is shown by different diameter of the tube (Figure 7). Energy with respect to different tubes is shown below along crystallographic b-direction (Supporting Information Figure S6). The interaction energy is small and there is little scope of slippage due to the interaction of the Boc *t*-butyl, Phe side chains and methyl-3-aminocrotonate in the multi layer sheets, which developed a brittle crystal.

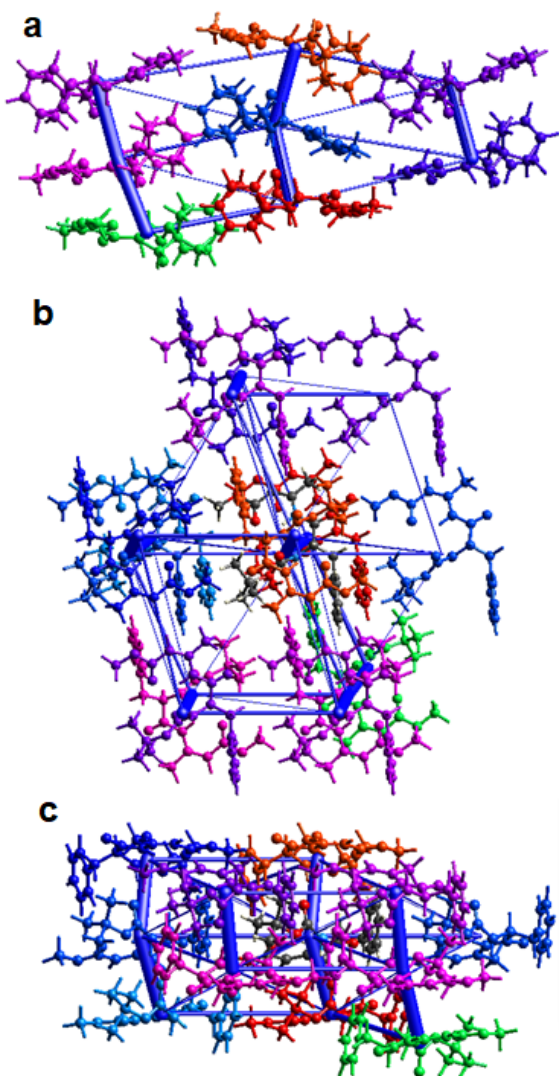


**Figure 7.** Three-dimensional topologies of energy framework for  $\alpha,\beta$ -hybrid peptide **1** viewed along the (a)  $a$  axis, (b)  $b$  axis, and (c)  $c$  axis.

## EXPERIMENTAL SECTION

**General:** L-Phe, methylacetoacetate and ammoniumformate were purchased from Sigma Chemicals. N-hydroxybenzotriazole (HOBt) and N,N'-dicyclohexylcarbodiimide (DCC) were purchased from SRL.

**Peptide Synthesis:** See Supporting Information.

**NMR Experiments:** The NMR experiments (1–10 mM in  $\text{CDCl}_3$ ) were carried out on Bruker 500 MHz spectrometers at 298 K.

**FT-IR Spectroscopy:** A Perkin Elmer Spectrum RX1 spectrophotometer has been used for the solid-state FT-IR experiments.

**Mass spectrometry:** The electrospray ionization (positive-mode) mass spectra of the compounds were recorded on a Q-T of Micro YA263 high-resolution (Waters Corporation) mass spectrometer.

**Single crystal X-ray diffraction study:** Intensity data of the  $\alpha,\beta$ -hybrid peptide **1** was collected with  $\text{MoK}\alpha$  radiation using

Bruker APEX-2 CCD diffractometer. Data were processed using the Bruker SAINT package and the structure solution and refinement procedures were performed using SHELX97. CCDC: 2151248 contain the supplementary crystallographic data for  $\alpha,\beta$ -hybrid peptide **1**.

**Field Emission Scanning Electron Microscopy:** The morphologies of the  $\alpha,\beta$ -hybrid peptide **1** crystal in a normal and broken state was examined by FE-SEM. A broken crystal was placed on the carbon tape and gold-coated. The micrographs were taken in an FE-SEM apparatus (ZEISS DSM 950 scanning electron microscope).

**Energy Frameworks:** CrystalExplorer 21.5 has been used to determine the aggregated pair-wise interaction energies (kJ/mol) and visualize the 3D topology energy frameworks of  $\alpha,\beta$ -hybrid peptide **1**. Intermolecular interaction energies was calculated using B3LYP/6-31G (d,p) dispersion corrected DFT model, with X–H bond lengths normalized to standard neutron diffraction values for the  $\alpha,\beta$ -hybrid peptide **1**.

## CONCLUSIONS

In summary, an unsaturated amino acid methyl-3-aminocrotonate has been developed and used to synthesized an  $\alpha,\beta$ -hybrid peptide. Eventually, we have explored the structure-mechanical property correlation of the  $\alpha,\beta$ -hybrid peptide. The monoclinic crystals with space group P 21/n are sensitive to external mechanical stress and brittle in nature. From POM and FE-SEM, the crystal is actually assembly of several sheet like structure. The single crystal X-ray analysis shows the existence of an unusual six-member intramolecular hydrogen bond and  $\alpha,\beta$ -hybrid peptide adopts a turn-like conformation. The  $\alpha,\beta$ -hybrid peptide forms a supramolecular twisted sheet-like structure through intermolecular hydrogen bonds and eventually a supramolecular multi layers structure along the crystallographic  $b$  and  $c$  directions in higher order assembly. From B3LYP/6-31G(d,p) dispersion corrected DFT model, although the interaction energy is small, there is no scope of slippage due to the interaction of the Boc *t*-butyl, Phe side chains and methyl-3-aminocrotonate in the multi layer sheets, which developed a brittle crystal. It is foreseen that the information included here may serve as the key elements for future development of ordered molecular materials.

## ACKNOWLEDGMENTS

This work is supported by CSIR, India (project No. 02(0404)/21/EMR-II). S. K. is thankful to CSIR, India for the senior research fellowship. We thank Dr. Rajesh Gonnade, National Chemical Laboratory, Pune, India for X-ray facilities.

## SUPPLEMENTARY INFORMATION

Supplementary material available: Supporting Information Figure S1-S5, Table S1-S2, Synthesis, and characterizations (Fig. S6-S8).

## CONFLICT OF INTEREST

Authors declared that no conflict of interest is there for this work.

## REFERENCES AND NOTES

1. E. Ahmed, D.P. Karothu, P. Naumov, Crystal adaptronics: mechanically reconfigurable elastic and superelastic molecular crystals. *Angew. Chem., Int. Ed.* **2018**, *57*, 8837-8846.
2. L. Zhu, R.O. Al-Kaysi, C.J. Bardeen, Photoinduced ratchet-like rotational motion of branched molecular crystals. *Angew. Chem., Int. Ed.* **2016**, *55*, 7073-7076.
3. P. Naumov, S. Chizhik, M.K. Panda, N.K. Nath, E. Boldyreva, Mechanically responsive molecular crystals. *Chem. Rev.* **2015**, *115*, 12440-12490.
4. L. Catalano, D.P. Karothu, S. Schramm, E. Ahmed, R. Rezgui, T.J. Barber, A. Famulari, P. Naumov, Dual-mode light Eduction through a plastically bendable organic crystal as an optical waveguide. *Angew. Chem., Int. Ed.* **2018**, *57*, 17254-17258.
5. S. Hayashi, S. Y. Yamamoto, D. Takeuchi, Y. Ie, K. Takagi, Creating elastic organic crystals of  $\pi$ -conjugated molecules with bending mechanofluorochromism and flexible optical waveguide. *Angew. Chem., Int. Ed.* **2018**, *57*, 17002-17008.
6. M. Owczarek, A. K. Hujzak, D. P. Ferris, A. Prokofjevs, I. Majerz, P. Szklarz, H. Zhang, A. A. Sarjeant, C. L. Stern, R. Jakubas, S. Hong, V. P. Dravid, J. F. Stoddart, Flexible ferroelectric organic crystals. *Nat. Commun.* **2016**, *7*, 13108.
7. R. Huang, C. Wang, Y. Wang, H. Zhang, Elastic self-doping organic single crystals exhibiting flexible optical waveguide and amplified spontaneous emission. *Adv. Mater.* **2018**, *30*, 1800814.
8. H. Liu, Z. Bian, Q. Cheng, L. Lan, Y. Wang, H. Zhang, Controllably realizing elastic/plastic bending based on a room temperature phosphorescent wave guiding organic crystal. *Chem. Sci.* **2019**, *10*, 227-232.
9. H. Wang, L. Deng, Q. Tang, Y. Tong, Y. Liu, Flexible organic single-crystal field-effect Eistor for ultra-sensitivity strain sensing. *IEEE Electron Device Lett.* **2017**, *38*, 1598-1601.
10. I. T. Desta, S. A. Chizhik, A. A. Sidelnikov, D. P. Karothu, E. V. Boldyreva and P. Naumov, Mechanically responsive crystals: analysis of macroscopic strain reveals "hidden" processes. *J. Phys. Chem. A*, **2020**, *124*, 300-310.
11. S. Saha, G. R. Desiraju, Trimorphs of 4-bromophenyl 4-bromobenzoate. Elastic, brittle, plastic. *Chem. Commun.*, **2018**, *54*, 6348-6351.
12. T. Kim, L. Zhu, L. J. Mueller and C. J. Bardeen, Mechanism of photoinduced bending and twisting in crystalline microneedles and microribbons composed of 9-methylanthracene. *J. Am. Chem. Soc.*, **2014**, *136*, 6617-6625.
13. T. Kim, M. K. Al-Muhanna, S. D. Al-Suwaidan, R. O. Al-Kaysi and C. J. Bardeen, Photoinduced curling of organic molecular crystal nanowires. *Angew. Chem. Int. Ed.*, **2013**, *52*, 6889-6893.
14. S. Saha and G. R. Desiraju, Crystal engineering of hand-twisted helical crystals. *J. Am. Chem. Soc.*, **2017**, *139*, 1975-1983.
15. S. Kobatake, S. Takami, H. Muto, T. Ishikawa and M. Irie, Rapid and reversible shape changes of molecular crystals on photoirradiation. *Nature*, **2007**, *446*, 778-781.
16. A. Priimagi, C. J. Barrett and A. Shishido, Recent twists in photoactuation and photoalignment control. *J. Mater. Chem. C*, **2014**, *2*, 7155-7162.
17. N. K. Nath, L. Pejov, S. M. Nichols, C. Hu, N. Saleh, B. Kahr and P. Naumov, Model for Photoinduced bending of slender molecular crystals. *J. Am. Chem. Soc.*, **2014**, *136*, 2757-2766.
18. A. G. Shtukenberg, Y. O. Punin, A. Gujral and B. Kahr, Growth actuated bending and twisting of single crystals. *Angew. Chem. Int. Ed.*, **2014**, *53*, 672-699.
19. G. R. Krishna, R. Devarapalli, G. Lal and C. M. Reddy, Mechanically Flexible organic crystals achieved by introducing weak interactions in structure: supramolecular shape synthons. *J. Am. Chem. Soc.*, **2016**, *138*, 13561-13567.
20. S. Das, A. Mondal and C. M. Reddy, Harnessing molecular rotations in plastic crystals: a holistic view for crystal engineering of adaptive soft materials. *Chem. Soc. Rev.*, **2020**, *49*, 8878-8896.
21. U. Ramamurty and J. -i. Jang, Nanoindentation for probing the mechanical behavior of molecular crystals—a review of the technique and how to use it. *CrystEngComm*, **2014**, *16*, 12-23.
22. B. P. A. Gabriele, C. J. Williams, D. Stauffer, B. Derby and A. J. Cruz-Cabeza, Brittle behavior in aspirin crystals: evidence of spalling fracture. *Cryst. Growth Des.*, **2021**, *21*, 1786-1790.
23. D. Haldar, S.K. Maji, M.G.B. Drew, A. Banerjee, A. Banerjee, Self-assembly of a short peptide monomer into a continuous hydrogen bonded supramolecular helix: the crystallographic signature. *Tetrahedron letters*, **2002**, *43*, 5465-5468
24. A.K. Das, A. Banerjee, M.G.B. Drew, S. Ray, D. Haldar, A. Banerjee, Can a consecutive double turn conformation be considered as a peptide based molecular scaffold for supramolecular helix in the solid state? *Tetrahedron*, **2005**, *61*, 5027-5036.
25. A. Banerjee, S.K. Maji, M.G.B. Drew, D. Haldar, A. Banerjee, An amyloid-like fibril forming antiparallel supramolecular  $\beta$ -sheet from a synthetic tripeptide: a crystallographic signature. *Tetrahedron letters*, **2003**, *44*, 6741-6744.
26. I. L. Karle, J. L. Flippen-Anderson, K. Uma and P. Balaram, Peptide mimics for structural features in proteins. Crystal structures of three heptapeptide helices with a C-terminal 6 $\rightarrow$ 1 hydrogen bond. *Int. J. Peptide Protein Res.*, **1993**, *42*, 401-410.
27. M.A. Spackman, J.J. McKinnon, Fingerprinting intermolecular interactions in molecular crystals. *CrystEngComm*, **2002**, *4*, 378-392.
28. M.J. Turner, S.P. Thomas, M.W. Shi, D. Jayatilaka, M.A. Spackman, Energy frameworks: insights into interaction anisotropy and the mechanical properties of molecular crystals. *Chem. Commun.*, **2015**, *51*, 3735-3738.
29. S.P. Thomas, M.W. Shi, G.A. Koutsantonis, D. Jayatilaka, A.J. Edwards, M.A. Spackman, The elusive structural origin of plastic bending in dimethyl sulfone crystals with quasi-isotropic crystal packing. *Angew. Chem. Int. Ed.*, **2017**, *56*, 8468-8472.
30. C. F. Mackenzie, P. R. Spackman, D. Jayatilaka and M. A. Spackman, Crystal Explorer model energies and energy frameworks: extension to metal coordination compounds, organic salts, solvates and open-shell systems. *IUCrJ*, **2017**, *4*, 575-587.